Exploring Practical Aspects of the FSK Modulation with Non-Coherent Matched Filter Detection

Dayan Adionel Guimarães, *Member, IEEE* and Rausley A. A. de Souza, *Member, IEEE*
National Institute of Telecommunications – Inatel. Santa Rita do Sapucaí, MG, Brazil.
e-mail: {dayan, rausley}@inatel.br

***Abstract*—This tutorial paper aims to contribute with the understanding of the non-coherently-detected frequency-shift keying (FSK) modulation from a practical standpoint. Specifically, the performances of a non-coherent correlator receiver and a non-coherent matched filter receiver simulated from a realistic implementation-oriented model are compared with theoretical results. It is shown that the matched filter receiver can achieve superior performances under the adoption of the realistic model. This result is credited to a noise variance reduction in the decision variable, which is caused by the low-pass filters present in the envelope detectors. In order to further support this result, a background material revisiting some concepts about optimality criteria for receiver design is also provided in this paper. Based on this material, it is highlighted that the performance of a receiver designed under a given optimality criterion may not be eventually optimal due to approximations adopted in the mathematical derivation of the optimum symbol decision rule. Moreover, it is emphasized that a receiver can be better in terms of one performance metric if it was not designed to be optimum with respect to that performance metric.**

***Index Terms*—Digital modulation, frequency-shift keying, correlator receiver, matched filter receiver, non-coherent detection, statistical decision theory.**

I. Introduction

It is well known that, in a digital communication system, the transmitted signal can undergo phase changes when traveling through the channel. This change can be produced, for instance, by the combination of the channel fading and propagation delay. To detect the transmitted signal, the receiver must be fed by a local carrier with a phase that mimics any phase change caused by the channel. In other words, carrier synchronization between the transmitter and the receiver must be guaranteed. Any modulation that makes use of this detection approach is said to be *coherently detected*. On the other hand, *non-coherently detected* modulations do not need carrier synchronization.

Coherent detection is performed at a cost, that is, the receiver must be equipped with a carrier recovery circuitry, which increases system complexity and may eventually increase equipment size and power consumption. Additionally, since there is no ideal carrier recovery circuit, no practical digital coherent communication system will work under perfect phase coherence. As a consequence, a performance penalty is expected and unavoidable. Non-coherent detection is simpler, but it suffers from performance degradation when compared with coherent detection. Nonetheless, this difference can be small in practice for some modulation schemes due to the specifics of the modulation and due to the penalty caused by imperfections in the carrier recovering process of coherently-detected modulations.

The frequency-shift keying (FSK) [1], [2] is a digital modulation with numerous applications, for example in the recently proposed physical layer network coding, as the main modulation of cordless, paging, facsimile and some telemetry systems modulation used in the control channel transmissions of some cellular systems, as one of the modulation formats available in many digital radio systems, and as an alternative modulation scheme adopted in modern underwater and powerline communication systems, just to name a few. [3]–[11]

In this paper, some practical aspects of the FSK modulation with non-coherent matched filter (MF) detection are explored, aiming at contributing to a deeper understanding about this modulation. To this end, the receiver is modeled adopting an implementation-oriented approach, i.e. the receiver blocks closely mimic the behavior of the corresponding parts in a real receiver. It is first shown that the performance of the receiver can be very close to the theoretical one, in spite of the imperfections that may take place in its construction, mainly related to the envelope detector [2]. Additionally, it is shown that the low-pass filters that are part of the envelope detectors can introduce intersymbol interference (ISI), but the negative effect of ISI can be surpassed by the positive effect of noise reduction in the decision variable, which is also caused by these filters. This results in a performance very close to, or even better than the theoretical performance of the optimum receiver. To justify the observations and to give to the paper a self-contained and didactic strength, it is also provided a background material revisiting some optimality criteria for receiver design, based on the statistical decision theory. From the reported results and based on this background material, it is highlighted the known fact that the performance of a receiver designed under some optimality criterion may not be eventually optimal due to approximations adopted in the mathematical derivation of the optimum decision rule. It is also highlighted that a receiver can be better in terms of one performance metric if it was not designed to be optimum with respect to that performance metric.

It is worth mentioning that the approach adopted here for studying the non-coherent detected FSK modulation can be used as a laboratory activity in basic digital communication courses.

The remaining of the paper is organized as follows: Section

Data de submissão: 30/12/2014. Data de aceitação: 14/04/2015.

II is devoted to a brief summary of some optimality criteria that can be used for receiver design. In Section III, some basics about the FSK modulation are revisited. The non-coherent detection of FSK signals based on the MF approach is treated in Section IV, where the analysis of the envelope detection is addressed from the perspective of intersymbol interference and noise variance reduction in the decision variable. Section V provides numerical results and discussions and Section VI concludes the paper.

II. Optimality Criteria for Receiver Design

In this section are summarized some optimality criteria used to design receivers for digital communications. Only the main conclusions considered to be sufficient to understand the meaning of what is meant to be optimized in each criterion are addressed. In other words, the only concern in this section is about the meaning for goodness in each design rule. The material presented here is strongly based upon the classical book by R. N. McDonough and A. D. Whalen [12], where a vast and deeper treatment of such topics and related ones can be found.

A. Maximum a Posteriori Criterion

The criterion of goodness for the *maximum a posteriori* (MAP) *criterion* receiver is to select the signal with maximum probability of having been sent (maximum posterior probability), given the observed decision variable. In a binary hypothesis testing, this criterion will result in a likelihood ratio test in which the likelihood ratio (which depends on the *a priori* probabilities of the hypotheses) is compared to 1. To apply the MAP rule theses probabilities must be known and the hypotheses must be *simple*, which means that there is no unknown parameter in the involved densities. The MAP rule minimizes the probability of a wrong decision and, as a consequence, it minimizes the average probability of a symbol error in a digital communication system. If the *a priori* probabilities are equal, the MAP rule reduces to the so-called *maximum likelihood* (ML) decision criterion.

In its original form, the MAP rule does not apply to the non-coherent detection problem. In this case the hypothesis test will not be simple, i.e. it will depend on the unknown carrier phase parameter. A *composite* hypothesis test applies in this situation.

B. Neyman-Pearson Criterion

In the *Neyman-Pearson* (NP) *criterion*, the probability of false alarm or false positive (type I error) is chosen as large as it can be tolerated and the probability of missed detection or false negative (type II error) is minimized, which is equivalent to maximizing the probability of detection. Adapted to the binary communication problem, the Neyman-Pearson criterion can be stated as follows: choose the probability of deciding in favor of one signal (say, s_1) given the other signal (s_0) has been sent as large it can be tolerated and minimize the probability of deciding in favor of s_0 given s_1 has been sent. (The terminology reverses if it is chosen to regard s1 as having been sent in the type I error constraint). The NP is inherently a binary hypothesis test criterion in which the hypotheses must be simple, but there is no need (and no use) of *a priori* probabilities of the hypotheses. It can also be reduced to a likelihood ratio test that, differently from the MAP criterion, is compared to a threshold that now must be computed. This computation is needed because, in NP, one is interested in meeting one target type I error (from s_0 to s_1, for instance) and minimizing the type II error (from s_1 to s_0) by choosing the appropriate threshold and the appropriate separation between the conditional densities involved, which in turn is achieved by choosing an appropriate signal-to-noise ratio.

It is worth mentioning that the NP criterion is general with respect to the conditional densities involved, which means that these densities can be of different types.

C. Bayes Criterion

The Bayes criterion is perhaps the most general rule for decision formulation. In this criterion, costs are assigned to each possible outcome of the decision process. Then, taking into account the *a priori* probability of each hypothesis, the average cost over all possible decisions is minimized. A decision threshold results from this optimization problem. The Bayes rule ends up with a likelihood ratio test in which the decision threshold is a function of the *a priori* probabilities of the hypotheses and of the costs assigned to each possible decision. Since the Bayes criterion is also based on a likelihood ratio test, it is similar to the MAP and to the NP criterion. What differs these three rules are the different computations of the decision thresholds. In particular, the MAP rule is a special case of the Bayes rule when the difference between the cost assigned to the wrong decision and the one assigned to the correct decision is the same for all hypotheses. As an example, in a binary communication system there is no reason for not assigning the same cost (say, 1) for deciding in favor of one bit or another. Likewise, there is no reason for assigning a cost different from 0 for a correct decision. Thus, in this case the Bayes decision rule reduces to the MAP rule, i.e. it minimizes the probability of error.

D. Minimum Error Probability Criterion

From above one can conclude that the decision criterion that yields the minimum error probability can be built from the MAP rule (without any modification) and from the Bayes rule when the difference between the cost assigned to the wrong decision and the one assigned to the correct decision is the same for all hypotheses.

E. Minimax Criterion

In the minimax rule, the Bayes criterion is applied in such a way that costs are assigned to the decisions, but there is not enough information to assign assuredly-correct *a priori* probabilities to the hypotheses. These probabilities are nonetheless assigned, but in a way that minimizes the negative effects of wrong assignments. As a consequence of this strategy, the average cost is made constant (insensitive) with respect to

the prior probabilities. In other words, if the problem under consideration presents us with prior probabilities different from those previously assigned, this will not affect the overall penalty for the wrong assignment. Surprisingly, it can be shown [12, p. 171] that this approach corresponds to finding the prior probabilities that *maximizes* the minimum average Bayes cost. For example, in a binary communication system, if the costs of wrong decisions are assigned equal to 1 and those corresponding to correct decisions equal to 0, the minimax criteria will result in equal error probabilities of deciding in favor to one bit or another, which corresponds to prior probabilities equal to 1/2. The same assignments applied to a radar system will result in a false alarm probability (type-I error) equal to the missed-detection probability (type-II error).

F. Composite Hypothesis Test with Minimum Cost

In some cases, the hypotheses of interest are not simple, i.e. the probability density of the observed data is not completely known. Then, if the likelihood ratio for the observed data is formed, its value cannot be computed since this ratio involves unknown parameters. Hypothesis tests under this situation are called *composite hypothesis tests*. In the composite hypothesis test, the problem of unknown parameters is dealt with by applying the Bayes criterion briefly discussed in Section II-C, now averaging the cost also over the unknown parameters. This will result in the minimum probability of error receiver, but often leading to larger error probabilities when compared to the situation in which there is complete knowledge about the probability densities under consideration. When the costs are independent of the unknown parameters, but the density of theses parameters are known, the Bayes rule for composite hypotheses reduces to the Bayes rule for simple hypotheses.

It is a common procedure to use the observed data to estimate the unknown parameters and then use the estimates to form the likelihood ratio as if these parameters were the correct ones. This procedure is often called the *generalized likelihood ratio test*. [12, p. 430].

G. An Optimality Criteria for Detecting Signals with Unknown Carrier Phase

In has been shown in the previous subsection that the densities of the observed data under the hypothesis were allowed to have unknown parameters, but nonetheless these densities must be specified. The resulting receivers designed under the minimum cost test criteria (see II-F) are thus optimal on average, this average taken over the ensemble of the unknown parameters values. For instance, a usual approach for detecting signals with unknown phases is to assume that they are random variables with uniform probability density. As a consequence, the approach of minimum cost can be applied, i.e. the average cost of deciding in favor of each hypothesis is also averaged over the phase angles. The problem of non-coherently detecting an M-ary FSK signal falls into this approach [1, Appendix B.3]. In this case, the likelihoods conditioned on each possible transmitted symbol and on the unknown phase parameter are averaged over the uniform phase angles before used in the decision process, which turns out to be equivalent to a maximum *a posteriori* probability criterion. This means that the corresponding receiver minimizes the average probability of symbol error, which in this case is the average cost if it is considered that correct decisions have zero cost and incorrect ones have unitary costs.

III. A Review about the FSK Modulation and Detection

M-ary FSK modulations belong to the broader class of orthogonal signaling, in which the data bits are represented by M orthogonal symbols, each one carrying $k = \log_2 M$ bits.

To be non-coherently orthogonal in the signaling interval T, two cosine functions with different frequencies must satisfy

$$f_1 = \frac{m+n}{2T}\ , \quad f_2 = \frac{m-n}{2T} \quad \text{and} \quad f_1 - f_2 = \frac{n}{T} \tag{1}$$

where m and n are integers. Then, frequencies f_1 and f_2 must be integer multiples of $1/(2T)$ and their frequency separation must be an integer multiple of $1/T$ [1, p. 101]. Recall that the minimum tone separation of $1/T$ for non-coherent detection is twice the minimum tone separation for coherent detection.

Based on the observation of the received signal $x(t)$ corrupted by additive white Gaussian noise (AWGN) and with unknown carrier phase, the optimum decision rule [1, Appendix B] for equally-likely symbols corresponds to decide in favor of the i-th symbol if the decision variable

$$y_j = \sqrt{x_{\mathrm{c}j}^2 + x_{\mathrm{s}j}^2} \tag{2}$$

is maximum for $j = i$, where

$$x_{\mathrm{c}j} = \int_0^T x(t)\phi_{\mathrm{c}j}(t)dt, \quad x_{\mathrm{s}j} = \int_0^T x(t)\phi_{\mathrm{s}j}(t)dt \tag{3}$$

and where

$$\phi_{\mathrm{c}j}(t) = \sqrt{\frac{2}{T}}\cos\left(2\pi f_j t\right),\ \phi_{\mathrm{s}j}(t) = \sqrt{\frac{2}{T}}\sin\left(2\pi f_j t\right) \tag{4}$$

for $j = 1, 2, \ldots, M$, are the base functions. The above decision rule has been derived under the minimum risk likelihood ratio test criterion of a composite hypothesis test (see Section II-F), which means that the corresponding receiver minimizes the symbol error probability.

The structure that implements the optimum receiver for non-coherent detection of an M-ary FSK modulated signal decides in favor of the symbol that will cause the largest envelope y_j or, equivalently, the largest squared envelop y_j^2, computed from the outputs of correlators realized according to (3). This optimum receiver is shown in Fig. 1, considering equally-likely symbols with equal energies. This receiver is usually referred to as the correlator receiver. Two sample and hold (S&H) blocks are shown in each quadrature branch to explicitly produce the observed vector $\mathbf{x} = [x_{\mathrm{c}1}\, x_{\mathrm{s}1}\, x_{\mathrm{c}2}\, x_{\mathrm{s}2} \cdots x_{\mathrm{c}M}\, x_{\mathrm{s}M}]^{\mathrm{T}}$. In a more practical implementation, just one S&H is needed after each summation block to produce each decision variable y_j^2.

A non-coherent (or incoherent) MF followed by an envelope detector can replace each pair of quadrature correlations in Fig. 1 [12, pp. 256-258] [13, pp. 341-344] [14, pp. 471-477]. The

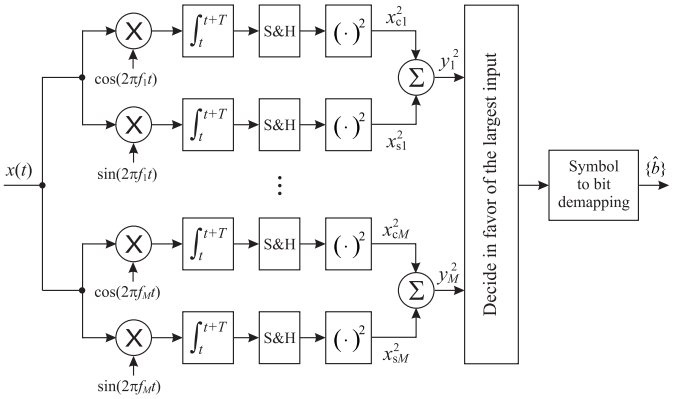

Fig. 1. Optimum non-coherent M-FSK receiver for equally-likely symbols.

sampled and held outputs of the M envelope detectors will also produce the decision variables $\{y_j^2\}$. This approach can simplify the receiver design and will be addressed here as a case study in the next section.

The average symbol error probability for a non-coherent detected M-ary FSK modulation, as provided by the optimum receiver in Fig. 1, is given by [1, Appendix B]

$$P_e = \sum_{i=1}^{M-1} \binom{M-1}{i} \frac{(-1)^{i+1}}{i+1} \exp\left[-\frac{i}{(i+1)}\frac{E_b}{N_0}\log_2 M\right]. \tag{5}$$

where E_b/N_0 is the ratio between the average energy per information bit and the noise power spectral density.

For $M = 2$, (5) specializes to

$$P_e = \frac{1}{2}\exp\left(-\frac{E_b}{2N_0}\right). \tag{6}$$

In what concerns the bit error probability, the following relation applies to any orthogonal signaling with equally-likely and equal energy symbols:

$$P_b = \frac{M}{2M-2}P_e. \tag{7}$$

As in the case of the coherent M-FSK, symbol and bit error probabilities for the non-coherent M-FSK are reduced with an increase in the value of M. However, the spectral efficiency reduces as M increases.

IV. Non-Coherent Matched Filter Approach

In this section it is analyzed the non-coherent demodulation of a binary continuous-phase FSK signal as a case study towards the main conclusions of the work. It has been adopted an experimental approach using VisSim/Comm, a communication's systems simulation software jointly developed by Visual Solutions, Inc. [1] and *Eritek, Inc.* [2]. The experiment is composed of two parts: the first one (Experiment 1) addresses some details behind the non-coherent detection of an FSK signal and aims at verifying the correct operation of the receiver. The second one (Experiment 2) considers a complete binary FSK (BFSK) modem with non-coherent detection, aiming at the performance assessment. The corresponding simulation files can be provided upon request to the authors.

[1] www.vissol.com
[2] www.eritek.com

A. Verifying the operation of the receiver via Experiment 1

A screenshot of the VisSim/Comm diagram for the first experiment is shown in Fig. 2. The "data bits generator" produces random bits or a single bit "1" or "0" at the middle of the simulation interval, according to the user selection. When the single bit transmission is selected, the modulator is switched off during the rest of the time. The selected data bit pattern is the input of a binary continuous-phase BFSK modulator, whose initial carrier phase can be configured by the user. The output of the modulator can be switched on or off. The selected input data bits and the BFSK modulated signal waveforms can be observed via the "time plot A" connected to the input and to the output of the modulator. The modulated signal goes through an AWGN channel whose gain and E_b/N_0 are configurable. The noise addition can also be enabled or disabled.

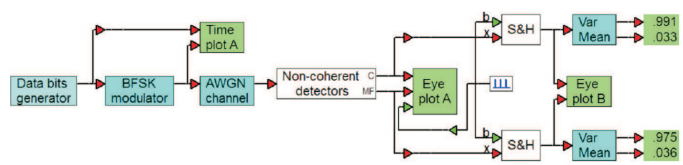

Fig. 2. VisSim/Comm diagram of the non-coherent BFSK system (Experiment 1).

The received signal enters two non-coherent BFSK detectors (inside the block "non-coherent detectors"). One of them was constructed according to Fig. 1 for $M = 2$, that is, by using two pairs of quadrature correlators, as shown in Fig. 3. The other detector, shown in Fig. 4, uses a non-coherent MF followed by an envelope detector replacing each pair of quadrature correlations. Each envelope detector was implemented by a rectifier (absolute value operation) followed by a low-pass filter. The filters were designed so as to minimize the mean square error between the actual and the ideal envelopes of the input signal.

It is possible to observe some waveforms processed by the matched-filter-based and by the correlation-based detectors through "time plot B" and "time plot C". The waveforms produced by these detectors are used to plot eye diagrams via "eye plot A" and then are converted into the decision variables by means of sample and hold (S&H) processes. Eye diagrams are also shown in the "eye plot B" after the decision variables

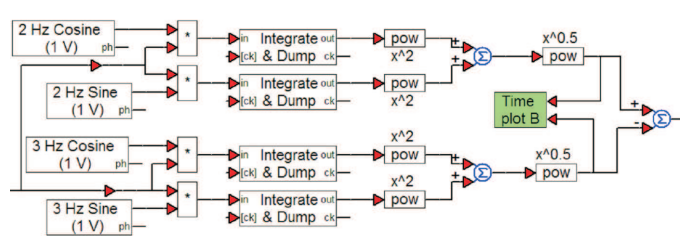

Fig. 3. VisSim/Comm diagram of the correlator-based detector.

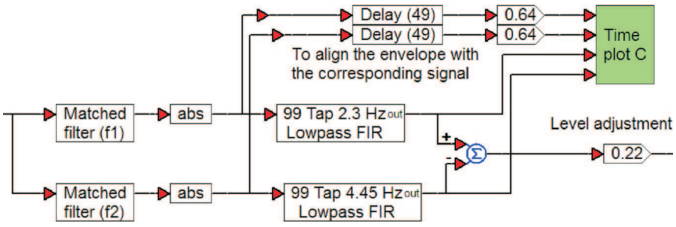

Fig. 4. VisSim/Comm diagram of the MF-based detector.

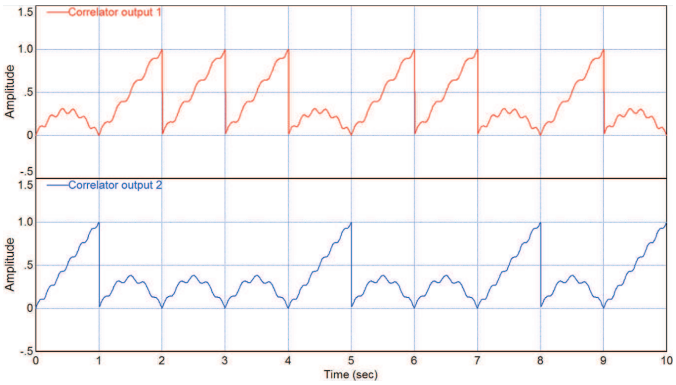

Fig. 5. Sample waveforms from "time plot B" in Fig. 3.

are formed. Additionally, estimations of the variance and mean of the decision variables are performed and displayed.

Observing Fig. 3 one can notice that the detector is producing the decision variables $\{y_j\}$ instead of the decision variables $\{y_j^2\}$; please see (2). The same is happening with the MF detector in Fig. 4. To verify the correct operation of the receiver, first observe a snapshot from the "time plot B" connected to the non-coherent correlation detector, as shown in Fig. 5. Notice that a maximum correlation produced in one arm (the upper waveform) corresponds to a zero correlation produced in the other (the lower waveform) for the same time instant (noise is disabled). This was expected and is a consequence of the use of an orthogonal signaling.

Now, as illustrated in Fig. 6, from the "time plot C" connected to the MF detector it is possible to see the waveforms (red and blue) at the output of the rectifiers (absolute value operations) and at the output of the low-pass filters of the envelope detectors (green and magenta). Observe that when the waveform in one arm exhibits a high peak, the other exhibits essentially zero and vice versa. Analogous to the case of the correlator receiver, this is a consequence of the use of an orthogonal signaling. Observe also that the envelopes are not equal to the ideal ones. To better illustrate this behavior, Fig. 7 shows responses of a non-coherent MF considering four values for the initial phase (indicated as *Theta*) of the corresponding tone, and the reception of just one pulse without noise. Observe that there exists a departure of the shape of the actual envelopes from the ideal (perfectly triangular) shape connecting the peaks of the rectified MF responses. Notice also that this departure is somewhat dependent of the amount of phase incoherence, which in this case is the value of the initial phase.

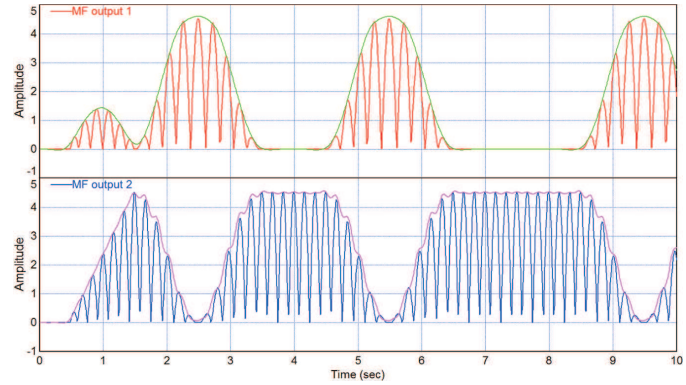

Fig. 6. Sample waveforms from "time plot C" in Fig. 4.

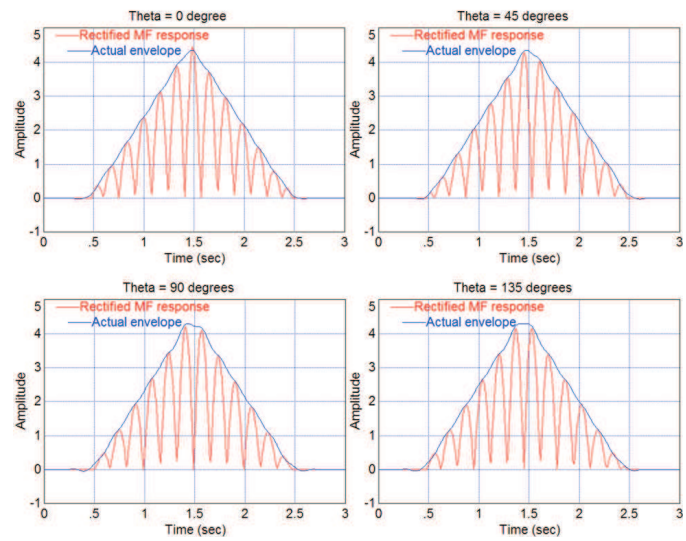

Fig. 7. Matched filter (MF) responses and envelopes for different initial phases.

Plots similar to those in Fig. 7 can be observed through the simulation by configuring the input data bit pattern for a "0" in the middle of the simulation interval, and then setting different initial carrier phases at the modulator.

It is known that the optimal sampling instant for a waveform coming from a correlator corresponds to a small interval before the integrator is dumped. When the waveform comes from a matched filter, the optimal sampling instant can be determined from an eye diagram; i.e. it corresponds to the instant of maximum vertical eye opening. This is verified thorough Experiment 1, via the"eye plot A" connected to the output of the detector. A realization of such diagram is shown in Fig. 8, where one can observe that sampling (black) is being realized at the maximum eye opening of the correlators' (red) and matched filters' (blue) waveforms. Noise has been disabled for plotting Fig. 8.

From above it can be attested that both detectors are working properly and that their performances can be fairly compared from this point on.

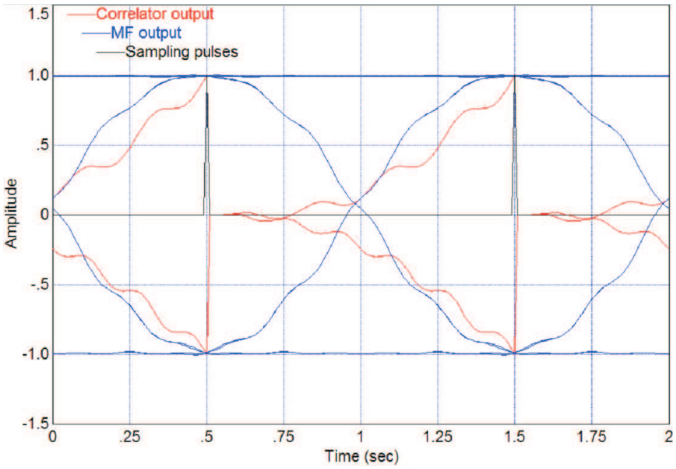

Fig. 8. Sample eye plots (blue for the MF receiver and red for the correlator) and sampling pulses (green) from "eye plot A" in Fig. 2.

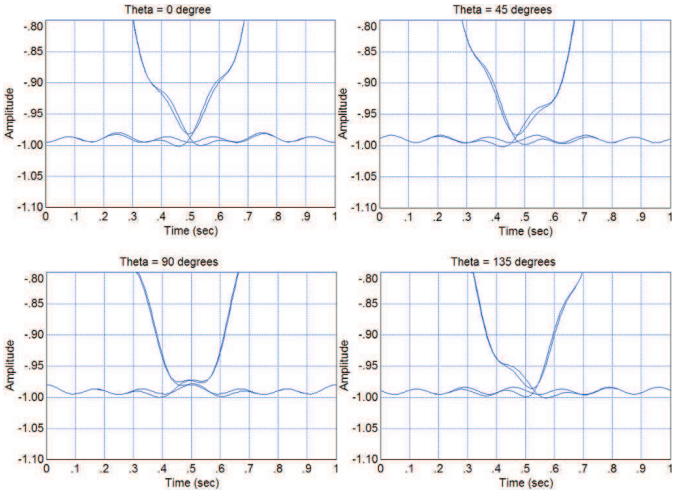

Fig. 9. Magnified eye plots for the MF receiver for some initial carrier phases at the modulator.

B. Unveiling Intersymbol Interference and Noise Reduction via Experiment 1

By magnifying the region of maximum opening of the MF output eye plot, as illustrated in Fig. 9 for the lower part of the eye opening, without noise, one can notice a small residual intersymbol interference, which is caused by the filters inside the envelope detectors (see Fig. 4). Different initial carrier phases for the modulator produce small, but noticeable different amounts of ISI at the best sampling instant (the center of all plots). The same ISI can also be observed from the"eye plot B", which shows the waveforms of the decision variables, that is, after sampling and holding the waveforms at the output of the MF and the correlation detectors.

Obviously, one would expect some degradation in the bit error rate (BER) due to the ISI. However, the degrading effect of ISI can be overcome by a performance improvement caused by the reduction in the noise variance present in the decision variable, which is also produced by the filters used in the envelope detectors. One can check this by turning the modulator OFF and enabling the AWGN in Experiment 1. For a more accurate observation, the simulation time must be increased to, say, $2,000$ seconds. All plots related to the receiver now show only the system responses to the noise. Particularly in the case of the eye diagrams that shows the decision variables, now they show only the noise that affects the decisions. Several estimations of the noise variance and mean were conducted and unveiled that, as expected, the mean approximates zero and the variance produced by the MF receiver is about 88% of the one obtained from the correlator receiver. If the amount of ISI is not enough to supplant this noise reduction, system performance in terms of BER will be better for the MF receiver. This will be verified in the next section.

V. Performance Results

The attention now is directed to Experiment 2, whose VisSim/Comm diagram is shown in Fig. 10. It corresponds to a non-coherent binary FSK modem in which the modulator is identical to the one used in Experiment 1. The transmitted

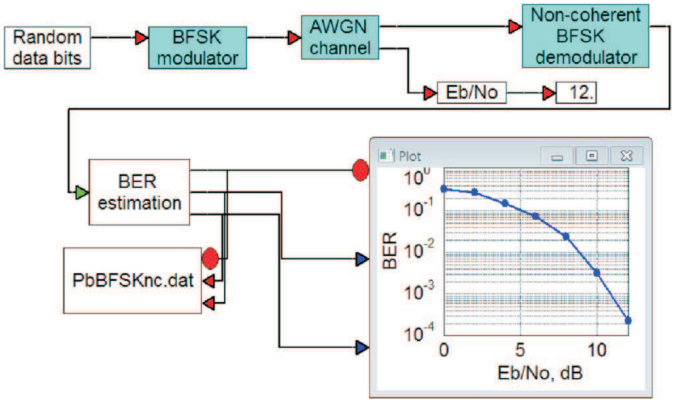

Fig. 10. VisSim/Comm diagram of the non-coherent BFSK modem (Experiment 2).

signal goes through an AWGN channel in which E_b/N_0 is automatically configured during the simulation to have the values 0, 2, 4, 6, 8, 10 and 12 dB. The channel gain can be configured by and noise addition can be disabled or enabled if desired. The received signal enters a non-coherent receiver in which a correlation-based or a matched-filter-based detection can be selected. The estimated bits are compared to the transmitted ones and a BER computation is performed. The values of E_b/N_0 and the BER results are stored as a ".dat" file so that the user can use them as desired.

Running the experiment with the default parameters allows one to obtain the system performance and compare the results with those obtained from (6). It would be expected a small degradation in performance of the non-coherent MF receiver when compared to the correlator receiver, since, for instance, the envelope detectors are not able to extract the exact actual envelope of the non-coherent MF output. This degradation, though, would become negligible for the nominal carrier frequency $f_c \gg 1/T$, which is the case in the majority of practical applications. On the other hand, it is shown here that the low-pass filters used in the envelope detectors are able to contribute to a reduction of the noise variance in

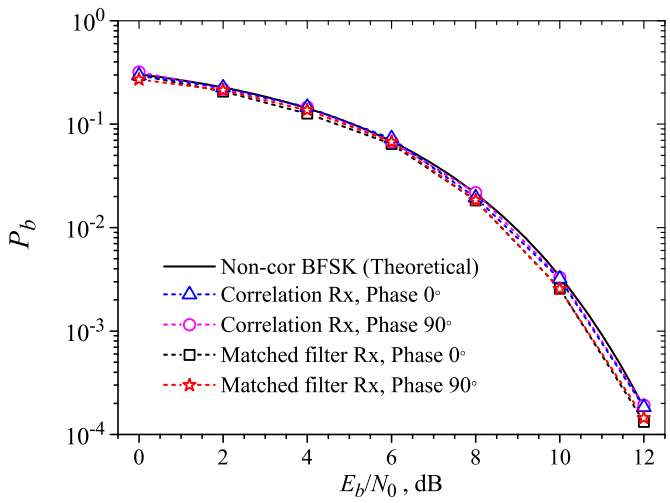

Fig. 11. Bit error probabilities for non-coherent BFSK for different initial carrier phases.

the decision variable, which is accompanied by some degree of intersymbol interference. This experiment can be used to show that the negative effect of ISI can be supplanted by the positive effect of noise reduction, leading to a performance improvement, even small, as compared to the non-coherent correlator receiver.

Fig. 11 shows some experimental BER results, where one can see a small difference in performance between the matched filter and the correlation approaches. Note also that in both cases the performances are practically insensitive to the initial carrier phase at the modulator. As expected, the error rates of the correlator receiver match the theoretical curve, since the modeling of this receiver within the VisSim/Comm environment does not consider any practical implementation aspect that would degrade its performance. From Fig. 11 it can also be observed that the MF receiver achieves error rates below the theoretical curve, which corresponds to the theoretical performance of the optimum receiver in Fig. 1 for $M = 2$.

VI. Concluding Remarks

In this paper, the performance of the frequency-shift keying (FSK) modulation with non-coherent matched filters was analyzed, comparing it with the performance of the correlator receiver and with theoretical results. It has been shown that, in spite of being theoretically equivalent to the correlator receiver, the MF receiver can achieve smaller error rates in a more realistic implementation-oriented approach in which the effects of a real envelope detector is taken into account. It has been demonstrated that this improved performance can be produced by a noise variance reduction in the decision variable, which is caused by the low-pass filters of the envelope detectors.

Somewhat surprisingly, the reported results unveiled that the MF receiver can achieve error rates below the one produced by the optimum receiver. Since the quadrature receiver was designed under the minimum error probability criterion (the same figure of merit used to assess its performance), it should not be surpassed by any other receiver. However, it is conjectured that the approximation of a low-pass filter by an integrator when obtaining the complex envelope from the real received signal [12, p. 256] has led to an optimal receiver rule that is in fact *approximately optimal*. This, in turn, has opened the possibility of having a receiver with better performance, justifying the results presented in this paper.

The approach adopted here for studying the non-coherent detected FSK modulation can be used as a laboratory activity in basic digital communication courses.

A natural deployment of the investigations discussed here is the development of a mathematical model of a non-coherent MF receiver for FSK signals with a real envelope detector and derive an expression for the bit error probability. This derivation would take into account both the ISI and noise reduction caused by the filters of the envelope detectors.

Acknowledgments

This work was partially supported by Finep/Funttel Grant No. 01.14.0231.00, under the Radiocommunication Reference Center (*Centro de Referência em Radiocomunicações* - CRR) project of the National Institute of Telecommunications (*Instituto Nacional de Telecomunicações* - Inatel), Brazil.

References

[1] F. Xiong, *Digital Modulation Techniques*. Norwood, MA, USA: Artech House, Inc. 2000

[2] D. A. Guimarães, *Digital Transmission: A Simulation-Aided Introduction with VisSim/Comm*. Berlin-Heidelberg, Germany: Springer-Verlag, Inc. 2009.

[3] Q. Yu, D. Zhang, H. Chen, and W. Meng, "Physical layer network coding systems with M-ary FSK modulation," *IEEE Trans. Veh. Technol.*, vol. PP, no. 99, pp. 1–1, Jan. 2015.

[4] Texas Instruments, "Implementation of FSK modulation and demodulation using CD74HC4046A," *Application Report*, SLAA618, Nov. 2013.

[5] Y. Li, X. Zhang, B. Benson, and R. Kastner, "Hardware implementation of symbol synchronization for underwater FSK," in *Sensor Networks, Ubiquitous, and Trustworthy Computing (SUTC), 2010 IEEE International Conference on*, 2010, pp. 82–88.

[6] G. Maniatis, K. Efstathiou and G. Papadopoulos, "Implementation of a bandwidth-efficient M-FSK demodulator for powerline communications," in *Solid-State Circuits Conference, 2003. ESSCIRC '03. Proceedings of the 29th European*, 2003, pp. 631.

[7] C. Temaneh-Nyah, and P. Chifamba, "An investigation of the effects of impulsive noise and channel distortion in narrow band power line communication," in *Digital Information, Networking, and Wireless Communications (DINWC), 2015 Third International Conference on*, 2015, pp. 16–21.

[8] N. Fasarakis-Hilliard, P. N. Alevizos, and A. Bletsas, "Coherent detection and channel coding for bistatic scatter radio sensor networking," *IEEE Trans. Comm.*, vol. PP, no. 99, pp. 1–1, Mar. 2015.

[9] A. Jerng, A. Truong, D. Wolday, E. Unruh, E. Landi, L. Wong, R. Fried, and S. Gibbons, "Integrated CMOS transceivers using single-conversion standard IF or low IF RX for digital narrowband cordless systems," in *Radio Frequency Integrated Circuits (RFIC) Symposium, 2002 IEEE*, 2002, pp. 111–114.

[10] S. Hong, M. Sagong, C. Lim, K. Cheun, and S. Cho, "FQAM : A modulation scheme for beyond 4G cellular wireless communication systems," in *Globecom Workshops (GC Wkshps), 2013 IEEE*, 2013, pp. 25–30.

[11] A. S. Walia, and E. M. Drakakis, , "A 13.56MHz short range telemetry link for the monitoring of incubated cell cultures," in *Engineering in Medicine and Biology Society, 2007. EMBS 2007. 29th Annual International Conference of the IEEE*, 2007, pp. 2273–2276.

[12] R. N. McDonough, A. D. Whalen *Detection of Signals in Noise*. (2nd edn). San Diego, CA, USA: Academic Press. 1995

[13] H. L. V. Trees, *Detection, Estimation and Modulation Theory*. Wiley Interscience. New York, 2001.

[14] M. B. Pursley, *Introduction to Digital Communications*. River, NJ, USA: Prentice-Hall, Inc. 2005.